Published in European Journal of Organic Chemistry, Vol. 2013, Issue 18, 2013, p. 3675-3684
which should be used for any reference to this work

Macrocyclic Effects in the Mesomorphic Properties of Liquid-Crystalline Pillar[5]- and Pillar[6]arenes

Iwona Nierengarten,[a] Sebastiano Guerra,[a,b] Michel Holler,[a] Lydia Karmazin-Brelot,[c] Joaquín Barberá,*[d] Robert Deschenaux,*[b] and Jean-François Nierengarten*[a]

Dedicated to Dr. Raymond Ziessel on the occasion of his 60th birthday

Keywords: Nanostructures / Macrocycles / Liquid crystals / Structure elucidation / Click chemistry

Whereas the reaction of 1,4-bis(2-bromoethyloxy)benzene (**4**) with paraformaldehyde in the presence of $BF_3{\cdot}Et_2O$ afforded exclusively the cyclopentameric pillar[5]arene derivative (**5**), both cyclopenta- and cyclohexameric macrocycles **5** and **6** were obtained when the reaction of **4** with paraformaldehyde was performed at 45 °C in $CHCl_3$ with $FeCl_3$ as the catalyst. Treatment of compounds **4**–**6** with sodium azide provided the corresponding polyazides, to which a cyanobiphenyl building block was subsequently grafted to generate model compound **1**, pillar[5]arene **2**, and pillar[6]arene **3**, bearing two, ten and twelve mesomorphic subunits, respectively. The liquid-crystalline and thermal properties of the compounds were investigated by polarized optical microscopy (POM), differential scanning calorimetry (DSC), and X-ray diffraction (XRD). Comparison of the liquid-crystalline properties of macrocycles **2** and **3** with those of **1** revealed the strong influence of the macrocyclic pillar[*n*]arene core on the mesomorphic properties. Whereas only a monotropic mesophase was observed for **1**, a broad enantiotropic mesophase was evidenced for both pillar[*n*]arene derivatives.

Introduction

One important aspect of modern chemistry is the synthesis of complex nanomolecules that exhibit specific properties for applications in materials science and biology.[1] It is clear that synthetic chemistry has played a major role in the recent advances of nanosciences and nanomedicine.[1] However, the preparation of complex nanostructures combining the required functional groups often remains difficult and requires a large number of synthetic steps, limiting both their accessibility and applicability. In this light, the design of versatile nanoscaffolds allowing for the grafting of one or more molecular entities to easily generate sophisticated nanomolecules has attracted enormous interest.[2–5] The recent development of efficient synthetic tools, namely the so-called 'click' reactions,[6] greatly facilitated the emergence of this field. As part of this research, we recently became interested in the use of a pillar[5]arene core as a nanoscaffold for the preparation of nanomaterials with a controlled distribution of functional groups on the macrocyclic framework.[7] Pillar[5]arenes are unique tubular-shaped compounds composed of 1,4-disubstituted hydroquinone subunits linked by methylene bridges in their 2,5-positions.[8–9] They are conveniently prepared from 1,4-dialkoxybenzene derivatives and paraformaldehyde in the presence of a Lewis acid catalyst.[10] Owing to the reversibility of the Friedel–Crafts reaction, the cyclooligomerization is thermodynamically driven, thus allowing pillar[5]arenes to be obtained in high yields.[11] The reaction conditions are, however, not compatible with a large variety of functional groups and the direct synthesis of pillar[5]arenes bearing sophisticated substituents is often not possible. The cyclization reaction is also sensitive to steric effects, and the presence of large substituents on the starting 1,4-dialkoxybenzene considerably lowers the yields.[10] This major problem was addressed by producing readily accessible pillar[5]arene derivatives bearing ten terminal groups, allowing their further functionalization to generate structurally more complex systems.[7,12] For example, we have developed a pillar[5]arene building block bearing ten peripheral azide func-

[a] Laboratoire de Chimie des Matériaux Moléculaires, Université de Strasbourg et CNRS (UMR 7509), Ecole Européenne de Chimie, Polymères et Matériaux,
25 rue Becquerel, 67087 Strasbourg Cedex 2, France
E-mail: nierengarten@unistra.fr
Homepage: http://www-ecpm.u-strasbg.fr/umr7509/WebLaboNierengarten.htm
[b] Institut de Chimie, Université de Neuchâtel,
Av. de Bellevaux 51, 2000 Neuchâtel, Switzerland
E-mail: robert.deschenaux@unine.ch
Homepage: http://www2.unine.ch/macrochem/page-6502.html
[c] Service de Radiocristallographie, Institut de Chimie, Université de Strasbourg,
1 rue Blaise Pascal, B.P. 296/R8, 67008 Strasbourg Cedex, France
[d] Departamento de Química Orgánica, Instituto de Ciencia de Materiales de Arágon, Universidad de Zaragoza – CSIC,
50009 Zaragoza, Spain
E-mail: jbarbera@unizar.es
Supporting information for this article is available on the WWW under http://dx.doi.org/10.1002/ejoc.201300356.

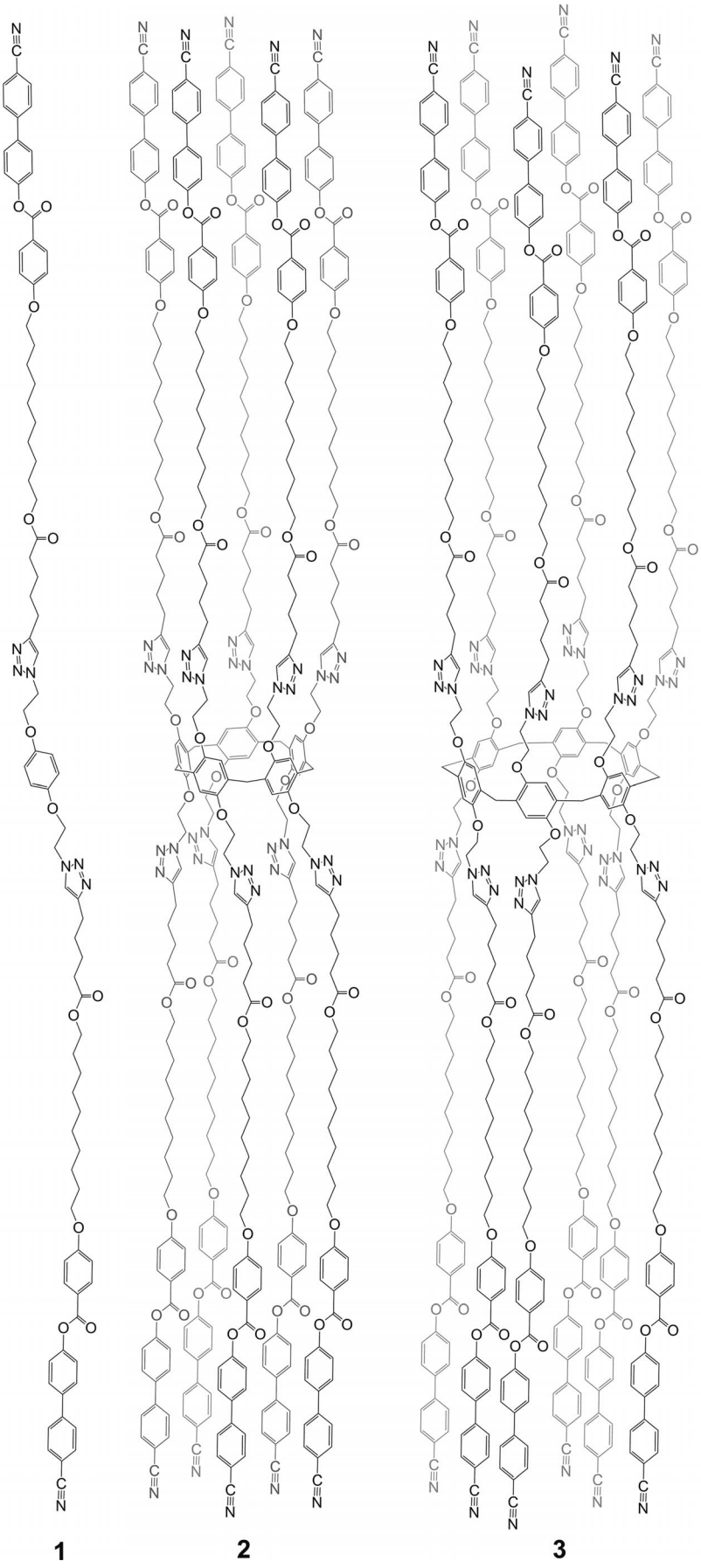

1 2 3

tions and shown that the copper-mediated Huisgen 1,3-dipolar cycloaddition of azides and alkynes resulting in 1,2,3-triazoles is an ideal tool with which to efficiently produce functionalized pillar[5]arenes.[7] This building block was decorated with cyanobiphenyl moieties, thus providing the first example of a liquid-crystalline pillar[5]arene (compound **2**).[7] Importantly, comparison of its mesomorphic properties with those of model compound **1** revealed a dramatic influence of the pillar[5]arene core. Indeed, whereas only a monotropic mesophase was observed for **1**, a broad enantiotropic mesophase was evidenced by linking together five linear subunits through the central macrocyclic pillar[5]arene core in **2**. Clearly, the macrocyclic core unit is capable of providing orientational and/or positional disorder within the smectic layers to prevent crystallization but also intermolecular π–π interactions between neighboring cores to stabilize the lamellar phase. An important question remains open however: Is this a general macrocyclic effect or does it result from the peculiar fivefold symmetry[13] of the pillar[5]arene core? To answer to this question, we now report a full account on this work, including the preparation of the corresponding sixfold symmetrical pillar[6]arene derivative **3**.

Results and Discussion

Synthesis

As shown in Scheme 1, pillar[5]arene derivative **5** was obtained from compound **4**. Treatment of **4** and paraformaldehyde with $BF_3{\cdot}Et_2O$ in 1,2-dichloroethane gave pillar[5]arene **5** in 40% yield.[14] Under these conditions, no trace of the corresponding pillar[6]arene derivative **6** could be detected.

Our initial attempts to prepare compound **6** from **4** under the conditions recently reported for the preferential preparation of pillar[6]arenes[15] ($FeCl_3/CHCl_3$) gave, at best, pillar[5]arene **5**, but no trace of the corresponding pillar[6]arene derivative **6**. The reaction conditions (solvent, catalyst, stoichiometry, temperature, reaction time) were thus systematically investigated in the particular case of starting material **4**. $FeCl_3$ and $CHCl_3$ appeared to be suitable, but both the temperature and the reaction time played an important role in the outcome of the reaction. The highest yields in pillar[6]arene were obtained when the reaction mixture was stirred for more than 3 d at temperatures higher than 45 °C. Furthermore, it was also noticed that the use of an excess of paraformaldehyde favored the formation of the cyclohexamer. Under optimized conditions, the reaction of **4** (1 equiv.) with a large excess of paraformaldehyde (5 equiv.) in the presence of $FeCl_3$ (0.2 equiv.) in $CHCl_3$ at 45 °C for 3 d gave both **5** and **6**. After work-up, compounds **5** and **6** were conveniently separated by column chromatography on SiO_2 and were isolated in 15 and 30% yield, respectively. The ^1H and ^{13}C NMR spectra of **5** and **6** are similar, but mass spectrometry provided definitive structural assignments.

For compound **6**, crystals suitable for X-ray crystal structure analysis were obtained by slow diffusion of hexane into a $CHCl_3$/PhCN (2:1) solution of **6**. As shown in Figure 1, **6** has a hexagon-like cyclic structure with two benzonitrile molecules included in its cavity. Interestingly, the relative orientation of the two PhCN molecules located in the same macrocycle is not antiparallel. The dipole moment thus generated may play an important role in the supramolecular organization within the crystal lattice (see above). The average bond angle for the methylene bridge in **6** is 114.2°, and differs significantly from both the ideal 109.5° angle for sp^3 hybridized carbons and the theoretical 120° internal angle for an unstrained hexagon. As a result, all the six aromatic subunits of **6** are slightly bent by about 1.6 to 4.2°. To further accommodate the strain across the methylene bridges, the six CH_2 moieties are not located in the same plane. Indeed, a deviation of 0.395 and 0.513 Å is observed for two methylene centers from the plane encompassing the four other centers. With its D_6-symmetrical structure, compound **6** is chiral and crystallizes as a racemate. Close inspection of the packing down the crystallographic *a* axis reveals alternating layers of both enantiomers (Figure 1, b). Layers a–b are related to the a′–b′ layers by a crystallo-

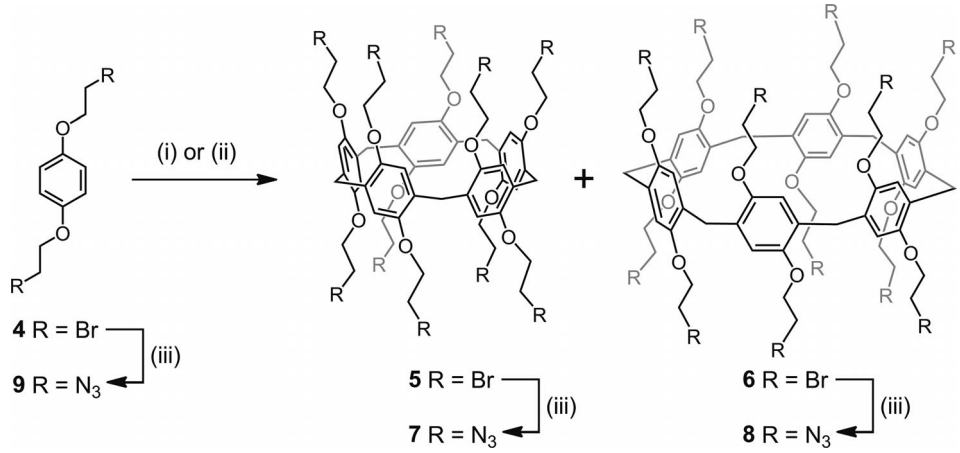

Scheme 1. Preparation of the azide building blocks. *Reagents and conditions:* (i) $(CH_2O)_n$, $BF_3{\cdot}Et_2O$, CH_2ClCH_2Cl, room temp. (**5**: 40%); (ii) $(CH_2O)_n$, $FeCl_3$, $CHCl_3$, 45 °C (**5**: 15%; **6**: 30%); (iii) NaN_3, DMF, room temp. (**7**: 97%; **8**: 98%; **9**: 92%).

graphic glide plane. The macrocycles are not oriented parallel to these planes but are significantly tilted. In this way, the PhCN molecules within one layer are oriented antiparallel with respect to the PhCN molecules of the neighboring layer. It is thus believed that the tilt of the pillar[6]arene cores results from interlayer dipole-dipole interactions. Within the layers, it can be noted that the pillar[6]arene molecules are organized in a hexagonal lattice (Figure 1, c). Even though the tilted orientation of the macrocycles prevents optimal overlap of the aromatic subunits, the establishment of notable intermolecular π–π interactions between neighboring macrocycles is clearly observed.

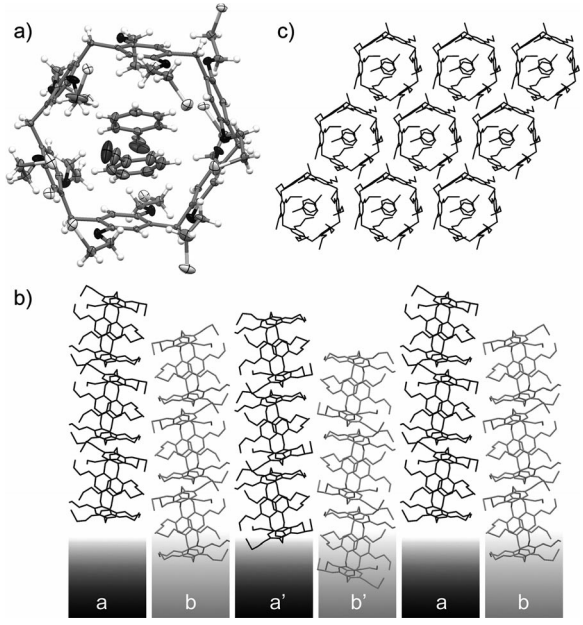

Figure 1. (a) ORTEP plot of the structure of **6**·$(PhCN)_2$ (thermal ellipsoids are shown at 50% probability level; C: gray; O: black, Br: pale gray; N: dark gray, H: white). (b) Stacking within the **6**·$(PhCN)_2$ lattice showing successive a/b/a′/b′ layers (view down the crystallographic *a* axis; the H atoms and the PhCN molecules are omitted for clarity). (c) Stacking within the **6**·$(PhCN)_2$ lattice revealing the hexagonal packing of the pillar[6]arene molecules within one layer (view down the crystallographic *b* axis; H are omitted for clarity).

The clickable pillar[5]- and pillar[6]arene building blocks **7**[16] and **8** were obtained by reaction of **5** and **6**, respectively, with sodium azide in *N*,*N*-dimethylformamide (DMF) at room temperature (Scheme 1). Similarly, treatment of **4** with NaN_3 afforded **9**, the precursor of **1**. Owing to the high number of azide residues, compounds **7**–**9** were handled with special care: upon evaporation, these polyazides were not dried under high vacuum and the use of metallic spatula was strictly avoided. Furthermore, these compounds were always prepared on small scales (<500 mg).

The functionalization of **7** and **8** with terminal alkynes under the typical copper-catalyzed alkyne-azide cycloaddition (CuAAC) conditions used for the functionalization of multi-azide cores[3] ($CuSO_4$·$5H_2O$, sodium ascorbate, CH_2Cl_2/H_2O) was first attempted from commercially available alkynes **10a**–**b** (Scheme 2). The clicked derivatives **11a**–**b** and **12a**–**b** were obtained in good yields. The structures of compounds **11a**–**b** and **12a**–**b** were confirmed by their ^1H and ^{13}C NMR spectra as well as by mass spectrometry. Inspection of the ^1H NMR spectra indicates the disappearance of the CH_2 azide signal at δ = 3.67–3.50 ppm (see the Supporting Information). IR data also confirmed that no azide residues (2089 cm^{-1}) remain in the final products (see the Supporting Information). Importantly, the ^1H NMR spectra of **11a**–**b** and **12a**–**b** show the typical singlet of the 1,2,3-triazole unit at δ = 7.8–7.9 ppm (see the Supporting Information).

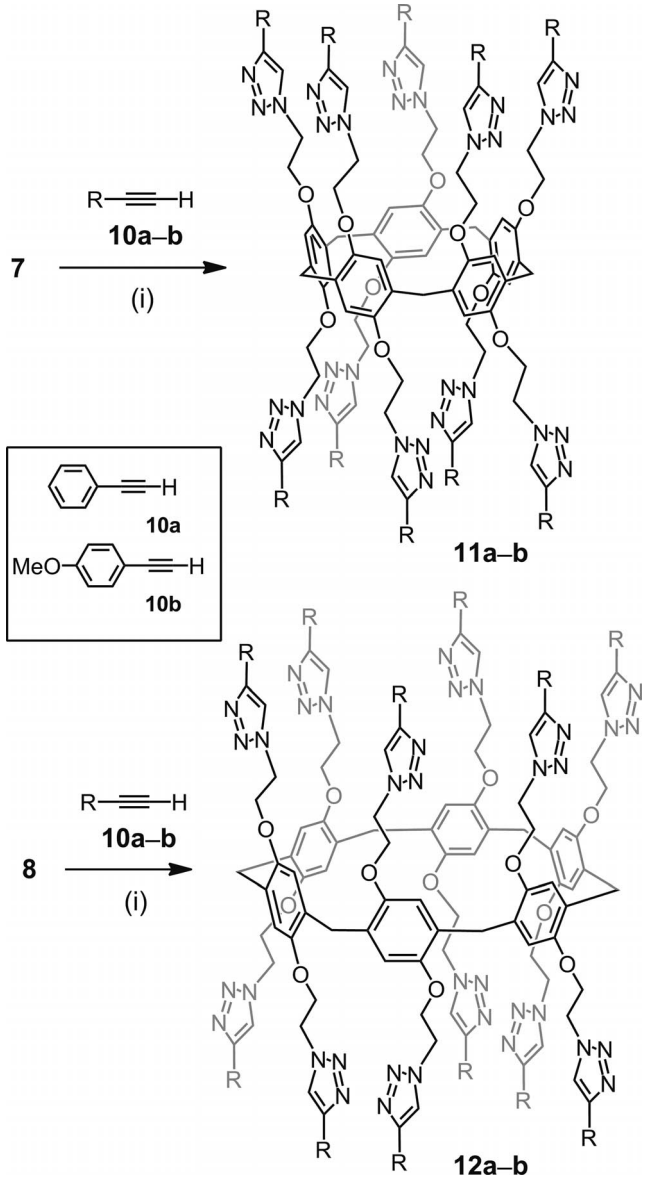

Scheme 2. Model CuAAC reactions from the pillar[*n*]arene building blocks **7** and **8**. *Reagents and conditions:* (i) $CuSO_4$·$5H_2O$, sodium ascorbate, CH_2Cl_2/H_2O, room temp. (**11a**: 60%; **11b**: 88%; **12a**: 84%; **12b**: 78%).

The reaction conditions used for the preparation of **11a**–**b** and **12a**–**b** were then applied to the mesomorphic subunit **15** (Scheme 3). Compound **15** was prepared by esterifica-

tion of 6-heptynoic acid (**14**) with alcohol **13** using 4-(dimethylamino)pyridinium *p*-toluenesulfonate (DPTS) and *N*,*N*′-dicyclohexylcarbodiimide (DCC). A mixture of **7** (1 equiv.), **15** (11 equiv.), $CuSO_4 \cdot 5H_2O$ (0.1 equiv.) and sodium ascorbate (0.3 equiv.) in CH_2Cl_2/H_2O (1:1) was vigorously stirred at room temperature for 24 h. After work-up and purification by column chromatography on SiO_2 followed by gel permeation chromatography (Biobeads SX-1, CH_2Cl_2), **2** was obtained in 81% yield. Similarly, reaction of polyazide **8** with alkyne **15** gave pillar[6]arene derivative **3** in 90% yield. Finally, model compound **1** was obtained in 91% yield from **9** and **15**. The structures of compounds **1**–**3** were confirmed by IR, ^1H and ^{13}C NMR spectroscopy, and by mass spectrometry. For all these compounds, the ^1H NMR spectra revealed one set of signals for the peripheral mesogenic moieties thus showing that they are all equivalent, in agreement with the symmetrical structures of compounds **1**–**3** (see the Supporting Information).

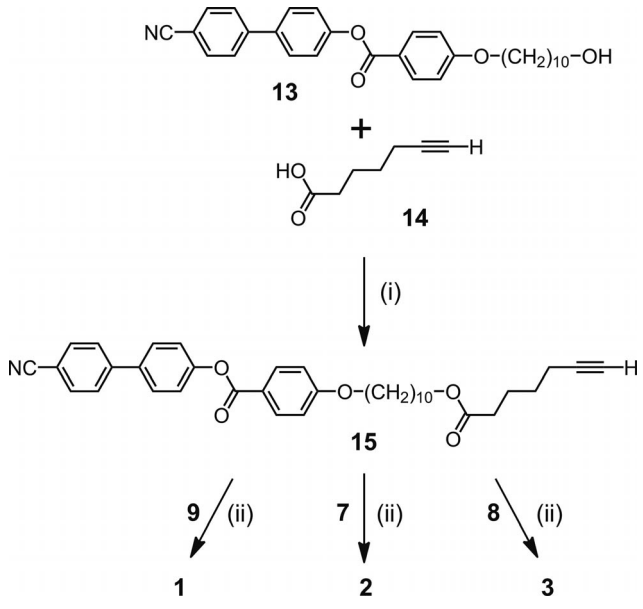

Scheme 3. Preparation of compounds **1**–**3**. *Reagents and conditions:* (i) DCC, DPTS, CH_2Cl_2, 0 °C to room temp. (91%); (ii) $CuSO_4 \cdot 5H_2O$, sodium ascorbate, CH_2Cl_2/H_2O, room temp. (**1**: 91%; **2**: 81%; **3**: 90%).

Liquid-Crystalline Properties

The liquid-crystalline and thermal properties of compounds **1**–**3** and **15** were investigated by polarized optical microscopy (POM), differential scanning calorimetry (DSC), and X-ray diffraction (XRD). Their thermal properties are summarized in Table 1.

On heating, model compound **1** melted at 145 °C from the crystalline state into the isotropic liquid. The formation of a monotropic smectic A phase (focal-conic fan texture, see the Supporting Information) was observed during the cooling run followed by crystallization of the sample. In contrast, the corresponding monomer **15** gave rise to an enantiotropic behavior with the observation of smectic A (114–156 °C) and nematic (156–158 °C) phases. Comparison of the thermal behavior of **1** and **15** reveals interesting features. Model compound **1** was isolated in a crystalline form, suggesting favorable intermolecular π-π interactions between the central aromatic parts of neighboring molecules. As a consequence of the strong intermolecular π-π interactions, the crystalline phase is stabilized and only a monotropic mesophase could form.

Table 1. Thermal properties of compounds **1**–**3** and **15** deduced from the POM and DSC investigations.

Compd.	Phase transition[a][b]	Temp. [°C][b]	Enthalpy changes ΔH [kJ mol^{-1}]
1	I → SmA	149	5.8
	SmA → Cr	125	119
2	(T_g: 32 °C); SmA → I	201	53
3	(T_g: 28 °C); SmA → I	209	60
15	Cr → SmA	114	64
	SmA → N	156	0.5
	N → I	158	0.1

[a] Cr: crystalline solid; SmA: smectic A phase; N: nematic phase; I: isotropic liquid, T_g: glass transition temperature. [b] Temperatures are given as the onset of the peak obtained during the second heating run. T_g values are determined during the first cooling run.

By linking together five or six linear subunits through a central macrocyclic pillar[*n*]arene core, the liquid-crystalline properties changed dramatically. Indeed, pillar[*n*]arene derivatives **2** and **3** gave rise to a broad enantiotropic smectic A phase (focal-conic fan texture and homeotropic areas, see the Supporting Information). Moreover, both **2** and **3** were obtained as glassy products and not as crystalline solids. Clearly, when compared with model compound **1**, crystallization is prevented by the macrocyclic structures linking the linear dimeric substructures. At the same time, the broad enantiotropic mesophases observed for **2** and **3** show that the macrocyclic core plays an important role regardless of its shape, i.e., pentagonal vs. hexagonal. It appears that the observed effect is not related to the fivefold symmetry of the central scaffold but is a general macrocyclic effect.[17]

To gain further understanding of this effect, high-temperature XRD measurements were carried out on the mesophases of cyclopentameric (**2**) and cyclohexameric (**3**) compounds and of precursor **15**. A full angular range 2θ = 1–40° was recorded and, for comparative purposes, the experiments were carried out in the three cases at the same temperature (130 °C). XRD measurements of the mesophase of **1** could not be performed due to its monotropic character and tendency to crystallize.

The X-ray patterns of the three compounds are consistent with a smectic A phase, as they contain a small-angle sharp maximum and a large-angle diffuse band. The sharp maximum is related to the layer order and from its angular position it is possible to deduce the interlayer spacing by using Bragg's law. The diffuse band arises from the lateral interferences between conformationally disordered hydrocarbon chains and denotes the absence of positional order of the mesogenic units within the layers.

Table 2 collects the spacing deduced from the XRD experiments for each compound. For **15**, the experimental

value (50 Å) is larger than the molecule length estimated from stereomodels for a fully-extended conformation (45 Å; Figure 2, a). A segment of 21 Å of that length corresponds to the rigid mesogenic unit and 24 Å corresponds to the hydrocarbon chains. However, the hydrocarbon chains are known not to be in their most-extended conformation in the mesomorphic state, and therefore the actual length of the molecule must be shorter than the theoretical value of 45 Å. To account for the experimental value of 50 Å, the molecules must adopt some kind of bilayer arrangement. This can be achieved if the molecules in the smectic layers adopt an alternating antiparallel orientation, so that the aliphatic regions are interpenetrated (Figure 2, a). It is probable that additional interdigitation takes place between adjacent layers due to the dipole–dipole interactions between the terminal cyano groups, a phenomenon described previously.[18]

Table 2. Structural data of compounds **2**, **3** and **15** deduced from the XRD measurements.

Compd.	Temp. [°C]	Mesophase	Measured spacing [Å]	Layer thickness [Å]
2	130	SmA	28	56
3	130	SmA	28	56
15	130	SmA	50	50

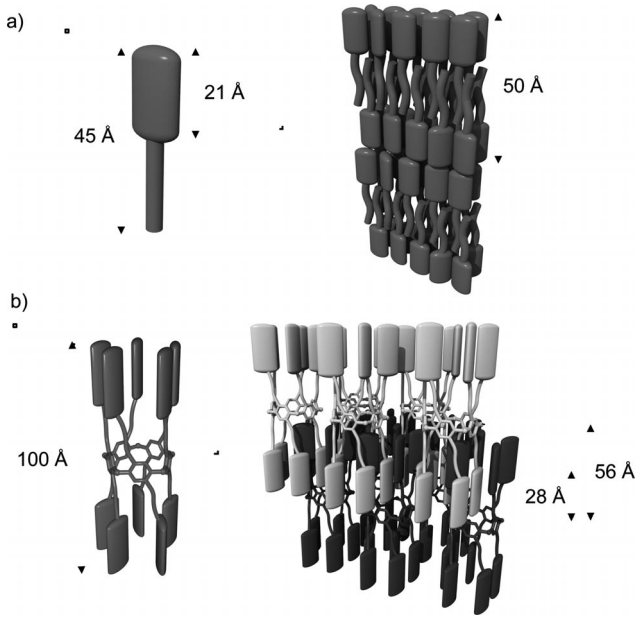

Figure 2. (a) Theoretical molecule length of **15** and postulated arrangement in the SmA phase. (b) Theoretical molecule length of **2** and postulated arrangement in the SmA phase; a similar organization is also postulated for **3**.

For compounds **2** and **3**, the experimentally-measured spacing was 28 Å. This value is too low for the layer thickness, taking into account that these molecules are much longer than molecules of **15**. Indeed the molecule length estimated with stereomodels for the fully-extended conformation of **2** and **3** is about 100 Å (Figure 2, b). Two conclusions arise from these results: (i) it is clear that some kind of interdigitation between molecules in neighboring layers takes place and that this reduces the effective layer thickness; (ii) the small-angle X-ray maximum corresponds to the second order layer reflection and thus the actual layer thickness is twice the value directly deduced from Bragg's law, that is 56 Å. This behavior in XRD has been previously reported and is related to the existence of some peculiarities in the supramolecular arrangement (see below).

Interdigitation in the mesophases of **2** and **3** must be a consequence of the particular molecular features of these mesomorphic compounds, in which the macrocyclic structure must provide a large space to accommodate the mesogenic units of the upper and lower layers. Considering that the mesogenic units in the pillar[*n*]arenes are able to mutually interpenetrate as described above for compound **15**, a fully-interdigitated structure can be proposed for the smectic layers of **2** and **3**. This high degree of interdigitation means that the mesogenic units of one particular layer are interpenetrated beyond the mesogenic units of the adjacent layer and are embedded in the aliphatic region of this adjacent layer (Figure 2, b).

The effective layer thickness estimated for the proposed structure can be as short as 58 Å (the molecule length, 100 Å, less twice the mesogenic unit length, 21 Å). Considering an additional shortening due to the conformational freedom of the aliphatic chains, which would reduce the effective periodicity to 56 Å, this is consistent with the observation of the second order reflection at 28 Å. The absence of the first order reflection may be related to the existence of a modulation of the electron density wave with a period equal to half the layer periodicity. Indeed, in the structure proposed for the smectic A phase of **2** and **3**, there are two maxima of the electron density along the normal to the layers, one of which corresponds to the macrocycles and the second corresponding to the interdigitated mesogenic units. The two regions are mutually spaced by half the full layer thickness. The same phenomenon has been described for side-chain polymers[19] and dendritic systems[20] with liquid crystal properties and is accounted for by the confinement of the polymer backbones or dendritic cores in a thin sublayer, thus producing an electron density maximum comparable to that of the mesogenic units. It is interesting to note that no differences are found between the supramolecular arrangement of **2** and **3**. It can be concluded that in both compounds a high degree of interpenetration between adjacent layers produces a good space filling and yields an efficient lateral arrangement of the mesogenic units in the SmA structure.

Conclusions

We have described the synthesis of pillar[5]arene **2** and pillar[6]arene **3**, bearing ten and twelve mesomorphic subunits, respectively. A broad enantiotropic mesophase has been evidenced for both macrocyclic compounds. The spe-

cific orientation of the cyanobiphenyl moieties attached on both rims of the macrocyclic core forces the system to adopt a supramolecular organization in which each smectic layer is interdigitated with its two neighboring layers. In this way, the mesophase is stable over a broad temperature range, which explains the macrocyclic effect observed for **2** and **3** when compared with model compounds **1** or **15**. Finally, it can be noted that pillar[*n*]arene derivatives are chiral. The present work paves the way for the preparation of optically pure derivatives with ferroelectric liquid crystalline properties. Work in this direction is underway in our laboratories.

Experimental Section

General: All reagents were used as purchased from commercial sources without further purification. Compounds **4**[14] and **13**[21] were prepared according to previously reported procedures. Evaporation and concentration were performed at water aspirator pressure and drying in vacuo at 10^{-2} Torr. Column chromatography was performed with silica gel 60 (230–400 mesh, 0.040–0.063 mm) purchased from E. Merck. Thin-layer chromatography (TLC) was performed on glass sheets coated with silica gel 60 F_{254} purchased from E. Merck (visualization by UV light). NMR spectra were recorded with a Bruker AC300 or AC400 with solvent peaks as reference. IR spectra were recorded with a Perkin–Elmer Spectrum One. Elemental analyses were performed by the analytical service of the ETH Zürich (Switzerland). MALDI-TOF and ESI mass spectra were recorded by the analytical service of the School of Chemistry (Strasbourg, France).

Liquid-Crystalline Properties: Transition temperatures (peak transitions) and enthalpies were determined with a differential scanning Mettler Toledo DSC 1 STAR calorimeter, under N_2, at a rate of 10 °C/min. The instrument was calibrated against indium. Optical studies were conducted with a Zeiss-Axioscope polarizing microscope equipped with a Linkam-THMS-600 variable-temperature stage. XRD measurements were carried out at high temperatures using a Pinhole camera (Anton-Paar) operating with a point focused Ni-filtered Cu-K_α beam. The sample was held in Lindemann glass capillaries (0.9 mm diameter) heated with a variable-temperature attachment. The diffraction patterns were collected on a flat photographic film mounted perpendicular to the X-ray beam.

Compound 5: $BF_3{\cdot}Et_2O$ (1.63 g, 11.5 mmol) was added to a stirred solution of **4** (3.73 g, 11.5 mmol) and paraformaldehyde (1.04 g, 34.5 mmol) in 1,2-dichloroethane (200 mL) at room temperature. After 3 h, the reaction mixture was concentrated. Column chromatography (SiO_2; cyclohexane/CH_2Cl_2, 1:1) gave **5** (1.54 g, 40%). The analytical data were identical to those reported in the literature for compound **5**.[14]

Compound 6: $FeCl_3$ (0.20 g, 1.24 mmol) was added to a stirred solution of **4** (2.00 g, 6.17 mmol) and paraformaldehyde (926 mg, 30.85 mmol) in $CHCl_3$ (90 mL) at 45 °C. After 72 h, the reaction mixture was concentrated. Column chromatography (SiO_2; cyclohexane/CH_2Cl_2, 1:1) followed by gel permeation chromatography (Biobeads SX-1; CH_2Cl_2) gave **5** (0.31 g, 15%) and **6** (0.62 g, 30%). Data for **6**: Colorless solid. ^{1}H NMR (CD_2Cl_2, 300 MHz): δ = 6.75 (s, 12 H), 4.14 (t, J = 6 Hz, 24 H), 3.86 (s, 12 H), 3.55 (t, J = 6 Hz, 24 H) ppm. ^{13}C NMR (CD_2Cl_2, 75 MHz): δ = 150.7, 129.0, 116.2, 69.5, 31.0, 30.9 ppm. MALDI-TOF-MS: *m*/*z* calcd. for $C_{66}H_{73}O_{12}Br_{12}$ [M + H]$^+$ 2017.12; found 2017.2. $C_{66}H_{72}Br_{12}O_{12}{\cdot}CH_2Cl_2$: calcd. C 38.30, H 3.55; found C 38.18, H 3.66.

Compound 7: A mixture of **5** (370 mg, 0.22 mmol) and NaN_3 (172 mg, 2.64 mmol) in DMF (10 mL) was stirred for 24 h at room temperature under Ar, then H_2O (45 mL) was added. The aqueous layer was extracted with Et_2O (3×). The combined organic layers were washed with water, dried with $MgSO_4$, filtered, and concentrated. Column chromatography (SiO_2; CH_2Cl_2) gave **7**[16] (278 mg, 97%) as a colorless solid that was used as received in the next step. ***Caution:*** *Owing to its high number of azide residues, this compound must be handled with special care. Upon evaporation, compound 7 has never been dried under high vacuum and the use of metallic spatula should be avoided. Furthermore, this compound has always been prepared on a small scale.* IR (neat): $\tilde{\nu}$ = 2089 (N_3) cm^{-1}. ^{1}H NMR (CD_2Cl_2, 300 MHz): δ = 6.94 (s, 10 H), 4.11 (t, J = 6 Hz, 20 H), 3.82 (s, 10 H), 3.67 (t, J = 6 Hz, 20 H) ppm.

Compound 8: A mixture of **6** (295 mg, 0.146 mmol) and NaN_3 (133 mg, 2.05 mmol) in DMF (10 mL) was stirred for 24 h at room temperature under Ar, then H_2O (50 mL) was added. The aqueous layer was extracted with Et_2O (3×60) and the combined organic layers were washed with water (2×), dried with $MgSO_4$, filtered and concentrated. Column chromatography (SiO_2; CH_2Cl_2) gave **8** (225 mg, 98%) as a colorless solid that was used as received in the next step. ***Caution:*** *Owing to its high number of azide residues, this compound must be handled with special care. Upon evaporation, compound **8** has never been dried under high vacuum and the use of metallic spatula should be avoided. Furthermore, this compound has always been prepared on a small scale.* IR (neat): $\tilde{\nu}$ = 2089 (N_3) cm^{-1}. ^{1}H NMR (CD_2Cl_2, 300 MHz): δ = 6.77 (s, 12 H), 3.99 (t, J = 6 Hz, 24 H), 3.91 (s, 12 H), 3.50 (t, J = 6 Hz, 24 H) ppm.

Compound 9: Prepared as described for **7** starting from **4** (389 mg, 1.2 mmol) and NaN_3 (195 mg, 3.0 mmol) in DMF (8 mL). Column chromatography (SiO_2; CH_2Cl_2) gave **9** (273 mg, 92%) as a colorless oil that was used as received in the next step. ***Caution:*** *Owing to its high nitrogen content, this compound must be handled with special care. Upon evaporation, compound **9** has never been dried under high vacuum and the use of metallic spatula should be avoided. Furthermore, this compound has always been prepared on a small scale.* IR (neat): $\tilde{\nu}$ = 2105 (N_3) cm^{-1}. ^{1}H NMR ($CDCl_3$, 300 MHz): δ = 6.88 (s, 4 H), 4.12 (t, J = 5 Hz, 4 H), 3.58 (t, J = 5 Hz, 4 H) ppm.

Compound 15: DCC (1.31 g, 6.36 mmol) was added to a solution of **13** (2.00 g, 4.24 mmol), **14** (640 mg, 5.09 mmol) and DPTS (1.25 g, 4.24 mmol) in anhydrous CH_2Cl_2 (100 mL) at 0 °C. After 1 h, the mixture was warmed slowly to room temperature and then stirred for 24 h at this temperature. The resulting mixture was evaporated and column chromatography (SiO_2; CH_2Cl_2) followed by precipitation (the sample was dissolved in CH_2Cl_2 and the resulting solution added dropwise to MeOH) and filtration gave **15** (2.23 g, 91%) as a colorless solid. ^{1}H NMR ($CDCl_3$, 400 MHz): δ = 8.20 (d, J = 9 Hz, 2 H), 7.76 (AA′XX′, $J_{A,X}$ = 9 Hz, 4 H), 7.68 (d, J = 9 Hz, 2 H), 7.38 (d, J = 9 Hz, 2 H), 7.03 (d, J = 9 Hz, 2 H), 4.11 (t, J = 7 Hz, 2 H), 4.10 (t, J = 6 Hz, 2 H), 2.38 (t, J = 7 Hz, 2 H), 2.26 (td, J = 7, 3 Hz, 2 H), 2.00 (t, J = 3 Hz, 1 H), 1.84 (m, 4 H), 1.61 (m, 4 H), 1.53 (m, 2 H), 1.37 (m, 10 H) ppm. ^{13}C NMR ($CDCl_3$, 100 MHz): δ = 173.5, 164.9, 163.7, 151.6, 144.9, 136.7, 132.7, 132.4, 128.4, 127.7, 122.61, 118.9, 114.4, 111.0, 84.0, 68.6, 68.4, 64.5, 33.8, 29.5, 29.45, 29.4, 29.2, 29.1, 28.7, 27.9, 26.0, 25.9, 24.1, 18.2 ppm. ESI-MS: *m*/*z* calcd. for $C_{37}H_{41}NO_5Na$ [M + Na]$^+$ 602.29; found 602.7. $C_{37}H_{41}NO_5$ (579.30): calcd. C 76.66, H 7.13, N 2.42; found C 76.42, H 7.17, N 2.39.

General Procedure for the Click Reactions: $CuSO_4{\cdot}5H_2O$ and sodium ascorbate were added to a mixture of azide **7**–**9** and the appropriate terminal alkyne in CH_2Cl_2/H_2O (1:1). The resulting mix-

ture was vigorously stirred at room temperature under Ar. After 24 h, H_2O was added, the aqueous layer was extracted with CH_2Cl_2 (3×), and the combined organic layers were dried ($MgSO_4$), filtered and concentrated. The product was then purified as outlined in the following text.

Compound 11a: Prepared from **7** (166 mg, 0.13 mmol), **10a** (146 mg, 1.43 mmol), $CuSO_4{\cdot}5H_2O$ (3.3 mg, 0.013 mmol) and sodium ascorbate (7.9 mg, 0.04 mmol) in CH_2Cl_2/H_2O (1:1, 6 mL). Column chromatography (SiO_2; CH_2Cl_2 containing 2% methanol) gave **11a** (180 mg, 60%) as a colorless glassy product. ^{1}H NMR (CD_2Cl_2, 300 MHz): δ = 7.92 (s, 10 H), 7.79 (m, 20 H), 7.38 (m, 20 H), 7.30 (m, 10 H), 6.55 (s, 10 H), 4.72 (m, 10 H), 4.57 (m, 10 H), 4.19 (m, 10 H), 4.05 (m, 10 H), 3.33 (s, 10 H) ppm. ^{13}C NMR ($CDCl_3$, 75 MHz): δ = 149.6, 147.8, 130.6, 129.0, 128.6, 128.3, 125.7, 120.3, 115.7, 67.2, 50.3, 29.7 ppm. ESI-TOF-MS: *m/z* calcd. for $C_{135}H_{120}N_{30}O_{10}$ $[M]^+$ 2320.9804; found 2320.9.

Compound 11b: Prepared from **7** (198 mg, 0.152 mmol), **10b** (221 mg, 1.67 mmol), $CuSO_4{\cdot}5H_2O$ (3.8 mg, 0.015 mmol) and sodium ascorbate (9.0 mg, 0.046 mmol) in CH_2Cl_2/H_2O (1:1, 8 mL). Column chromatography (SiO_2; CH_2Cl_2 containing 2% methanol) gave **11b** (350 mg, 88%) as a colorless glassy product. ^{1}H NMR (CD_2Cl_2, 300 MHz): δ = 7.83 (s, 10 H), 7.72 (d, J = 7 Hz, 20 H), 6.93 (d, J = 7 Hz, 20 H), 6.57 (s, 10 H), 4.72 (m, 10 H), 4.58 (m, 10 H), 4.19 (m, 10 H), 4.04 (m, 10 H), 3.78 (s, 30 H), 3.36 (s, 10 H) ppm. ^{13}C NMR ($CDCl_3$, 75 MHz): δ = 159.6, 149.5, 147.6, 128.6, 127.0, 123.3, 119.5, 115.6, 114.4, 67.2, 55.2, 50.3, 29.4 ppm. ESI-TOF-MS: *m/z* calcd. for $C_{145}H_{140}N_{30}O_{20}$ $[M]^+$ 2621.086; found 2621.1.

Compound 12a: Prepared from **8** (77 mg, 0.05 mmol), **10a** (66 mg, 0.65 mmol), $CuSO_4{\cdot}5H_2O$ (1.3 mg, 0.005 mmol) and sodium ascorbate (3.0 mg, 0.015 mmol) in CH_2Cl_2/H_2O (1:1, 8 mL). Column chromatography (SiO_2; CH_2Cl_2 containing 1.6% methanol) gave **12a** (114 mg, 84%) as a colorless glassy product. ^{1}H NMR (CD_2Cl_2, 300 MHz): δ = 7.91 (s, 12 H), 7.76 (d, J = 7 Hz, 24 H), 7.38 (m, 36 H), 6.55 (s, 12 H), 4.45 (br. s, 24 H), 4.06 (br. s, 24 H), 3.42 (s, 12 H) ppm. ^{13}C NMR ($CDCl_3$, 75 MHz): δ = 150.0, 147.8, 130.5, 128.9, 128.2, 127.8, 125.6, 120.6, 115.5, 67.1, 49.9, 31.0 ppm. MALDI-TOF-MS: *m/z* calcd. for $C_{162}H_{144}N_{36}O_{12}$ $[M]^+$ 2785.177; found 2785.9.

Compound 12b: Prepared from **8** (73 mg, 0.047 mmol), **10b** (81 mg, 0.61 mmol), $CuSO_4{\cdot}5H_2O$ (1.3 mg, 0.005 mmol) and sodium ascorbate (2.8 mg, 0.014 mmol) in CH_2Cl_2/H_2O (1:1, 8 mL). Column chromatography (SiO_2; CH_2Cl_2 containing 1.5% methanol) gave **12b** (115 mg, 78%) as a colorless glassy product. ^{1}H NMR (CD_2Cl_2, 300 MHz): δ = 7.81 (s, 12 H), 7.63 (d, J = 7 Hz, 24 H), 6.85 (d, J = 7 Hz, 24 H), 6.51 (br. s, 12 H), 4.46 (m, 24 H), 4.04 (m, 24 H), 3.75 (s, 36 H), 3.38 (s, 12 H) ppm. ^{13}C NMR (CD_2Cl_2, 75 MHz): δ = 160.0, 150.5, 147.8, 128.3, 127.0, 123.8, 120.3, 115.9, 114.6, 67.6, 55.6, 50.3, 29.8 ppm. MALDI-TOF-MS: *m/z* calcd. for $C_{174}H_{168}N_{36}O_{24}$ $[M + H]^+$ 3146.311; found 3146.0.

Compound 1: Prepared from **9** (72 mg, 0.288 mmol), **15** (418 mg, 0.720 mmol), $CuSO_4{\cdot}5H_2O$ (7 mg, 0.029 mmol) and sodium ascorbate (17 mg, 0.086 mmol) in CH_2Cl_2/H_2O (1:1, 10 mL). Column chromatography (SiO_2; CH_2Cl_2 containing 1.7% methanol) gave **1** (370 mg, 91%) as a colorless solid. IR (neat): $\tilde{\nu}$ = 2226 (C≡N), 1725 (C=O) cm^{-1}. ^{1}H NMR (CD_2Cl_2, 300 MHz): δ = 8.07 (d, J = 7 Hz, 4 H), 7.67 (AA′XX′, $J_{A,X}$ = 7 Hz, 8 H), 7.61 (d, J = 7 Hz, 4 H), 7.42 (s, 2 H), 7.26 (d, J = 7 Hz, 4 H), 6.93 (d, J = 7 Hz, 4 H), 6.73 (s, 4 H), 4.59 (t, J = 6 Hz, 4 H), 4.20 (t, J = 6 Hz, 4 H), 3.98 (t, J = 6 Hz, 4 H), 3.96 (t, J = 6 Hz, 4 H), 2.63 (m, 4 H), 2.25 (m, 4 H), 1.75 (m, 4 H), 1.60 (m, 8 H), 1.53 (m, 4 H), 1.41 (m, 4 H), 1.25 (m, 20 H) ppm. ^{13}C NMR ($CDCl_3$, 75 MHz): δ = 173.6, 164.8, 163.7, 152.71, 151.6, 144.8, 136.7, 132.6, 132.3, 128.3, 127.7, 122.6, 121.2, 118.9, 115.8, 114.4, 111.0, 68.4, 67.1, 64.5, 34.0, 29.5, 29.4, 29.3, 29.2, 29.1, 28.6, 26.0, 25.9, 25.3, 24.5 ppm. ESI-TOF-MS: *m/z* calcd. for $C_{84}H_{95}N_8O_{12}$ $[M + H]^+$ 1407.7069; found 1407.8. $C_{84}H_{95}N_8O_{12}$ (1407.71): calcd. C 71.67, H 6.73, N 7.96; found C 71.39, H 6.69, N 7.85.

Compound 2: Prepared from **7** (83 mg, 0.064 mmol), **15** (408 mg, 0.704 mmol), $CuSO_4{\cdot}5H_2O$ (2.0 mg, 0.007 mmol) and sodium ascorbate (4.0 mg, 0.019 mmol) in CH_2Cl_2/H_2O (1:1, 8 mL). Column chromatography (SiO_2; CH_2Cl_2 containing 2.5% methanol) followed by gel permeation chromatography (Biobeads SX-1; CH_2Cl_2) gave **2** (369 mg, 81%) as a colorless glassy product. IR (neat): $\tilde{\nu}$ = 2226 (C≡N), 1727 (C=O). ^{1}H NMR (CD_2Cl_2, 300 MHz): δ = 8.04 (d, J = 7 Hz, 20 H), 7.64 (AA′XX′, $J_{A,X}$ = 7 Hz, 40 H), 7.57 (d, J = 7 Hz, 20 H), 7.53 (s, 10 H), 7.23 (d, J = 7 Hz, 20 H), 6.89 (d, J = 7 Hz, 20 H), 6.56 (s, 10 H), 4.70 (m, 20 H), 4.20 (m, 10 H), 4.10 (m, 10 H), 3.94 (t, J = 6 Hz, 20 H), 3.91 (t, J = 6 Hz, 20 H), 3.21 (s, 10 H), 2.61 (m, 20 H), 2.19 (m, 20 H), 1.70 (m, 20 H), 1.56 (m, 60 H), 1.37 (m, 20 H), 1.22 (m, 100 H) ppm. ^{13}C NMR ($CDCl_3$, 75 MHz): δ = 173.5, 164.8, 163.7, 151.6, 149.4, 148.0, 144.8, 136.7, 132.6, 132.3, 131.5, 128.3, 127.7, 122.5, 121.3, 121.2, 118.8, 114.4, 111.0, 68.3, 67.1, 64.5, 50.1, 33.9, 29.7, 29.5, 29.4, 29.2, 29.1, 28.9, 28.6, 26.0, 25.9, 25.3, 24.5 ppm. MALDI-TOF-MS: *m/z* calcd. for $C_{425}H_{470}N_{40}O_{60}Na_3$ $[M + 3Na]^{3+}$ 2389.167; found 2388.8. $C_{425}H_{470}N_{40}O_{60}$ (7098.62): calcd. C 71.91, H 6.67, N 7.89; found C 71.66, H 6.84, N 7.62.

Compound 3: Prepared from **8** (70 mg, 0.045 mmol), **15** (60 mg, 0.59 mmol), $CuSO_4{\cdot}5H_2O$ (1.0 mg, 0.005 mmol) and sodium ascorbate (5.0 mg, 0.014 mmol) in CH_2Cl_2/H_2O (1:1, 14 mL). Column chromatography (SiO_2; CH_2Cl_2 containing 2.4% methanol) followed by gel permeation chromatography (Biobeads SX-1; CH_2Cl_2) gave **3** (345 mg, 90%) as a colorless glassy product. IR (neat): $\tilde{\nu}$ = 2226 (C≡N), 1726 (C=O). ^{1}H NMR (CD_2Cl_2, 300 MHz): δ = 8.10 (d, J = 7 Hz, 24 H), 7.71 (AA′XX′, $J_{A,X}$ = 7 Hz, 48 H), 7.64 (d, J = 7 Hz, 24 H), 7.51 (s, 12 H), 7.29 (d, J = 7 Hz, 24 H), 7.00 (d, J = 7 Hz, 24 H), 6.59 (br. s, 12 H), 4.55 (m, 24 H), 4.12 (m, 24 H), 4.00 (m, 48 H), 3.33 (br. s, 12 H), 2.61 (m, 24 H), 2.26 (m, 24 H), 1.79 (m, 24 H), 1.56 (m, 72 H), 1.44 (m, 24 H), 1.29 (m, 120 H) ppm. ^{13}C NMR ($CDCl_3$, 100 MHz): δ = 173.6, 164.9, 163.7, 151.6, 150.1, 148.0, 144.8, 136.7, 132.7, 132.4, 128.4, 127.7, 122.6, 121.2, 118.9, 114.4, 114.1, 111.0, 68.4, 67.3, 64.6, 49.9, 34.0, 29.5, 29.4, 29.3, 29.2, 29.0, 28.7, 26.1, 26.0, 25.4, 24.6 ppm. MALDI-TOF-MS: *m/z* calcd. for $C_{510}H_{565}N_{48}O_{72}$ $[M + H]^+$ 8519.241; found 8520.5. $C_{510}H_{564}N_{48}O_{72}$ (8518.23): calcd. C 71.91, H 6.67, N 7.89; found C 71.62, H 6.70, N 7.83.

X-ray Crystal Structure of Compound 6: Crystals suitable for X-ray crystal structure analysis were obtained by slow diffusion of hexane into a $CHCl_3$/PhCN solution of **6**. Data were collected at 173 K with a Bruker APEX-II Duo KappaCCD diffractometer (Mo-K_α radiation, λ = 0.71073 Å). The structure was solved by direct methods (SHELXS-97) and refined against F^2 using the SHELXL-97 software. The non-hydrogen atoms were refined anisotropically using weighted full-matrix least-squares on F^2. The H-atoms were included in calculated positions and treated as riding atoms using SHELXL default parameters. A semiempirical absorption correction was applied using SADABS in APEX2; transmission factors: T_{min}/T_{max} = 0.2341/0.3227. Crystallographic data: formula: $C_{66}H_{72}O_{12}Br_{12}{\cdot}(C_7H_5N)_2$ (M = 2222.40 g mol^{-1}); colorless crystal; 0.35× 0.30× 0.25 mm; crystal system: monoclinic; space group $P2_1/c$; a = 13.8558(7) Å; b = 50.521(3) Å; c = 13.5767(7) Å; β = 119.0850(10)°; V = 8305.4(7) Å^3; Z = 4; F(000) = 4368; a total of 71506 reflections collected; 1.90° < θ < 27.97°, 18075 independent

reflections with 13909 having $I > 2\sigma(I)$; 955 parameters; Final results: $R_1(F^2)$ = 0.0653; $wR_2(F^2)$ = 0.1217, Goof = 1.113. CCDC-923081 contains the supplementary crystallographic data for this paper. These data can be obtained free of charge from The Cambridge Crystallographic Data Centre via www.ccdc.cam.ac.uk/data_request/cif.

Supporting Information (see footnote on the first page of this article): Spectroscopic data and HPLC traces for the new compounds, DSC thermograms, and POM pictures of the liquid crystalline derivatives.

Acknowledgments

This research was supported by the University of Strasbourg, the Centre Nationale de la Recherche Scientifique (CNRS), the Spanish project CTQ2012-35692, the FEDER founds and the Swiss National Science Foundation (grant number 200020-140298). I. N. thanks the Agence National de la Recherche (ANR) and S. G. the Swiss National Science Foundation for postdoctoral fellowships. The authors further thank M. Schmitt for the NMR measurements.

[1] K. E. Geckeler, H. Nishide (Eds.), *Advanced Nanomaterials*, Wiley-VCH, Weinheim, Germany, **2010**.

[2] For general examples, see: a) L. M. Campos, K. L. Killops, R. Sakai, J. M. J. Paulusse, D. Damiron, D. E. Drockenmuller, B. M. Messmore, C. J. Hawker, *Macromolecules* **2008**, *41*, 7063–7070; b) A. S. Goldmann, A. Walther, L. Nebhani, R. Joso, D. Ernst, K. Loos, C. Barner-Kowollik, L. Berner, A. H. E. Muller, *Macromolecules* **2009**, *42*, 3707–3714; c) L. Nurmi, J. Lindqvist, R. Randev, J. Syrett, D. M. Haddleton, *Chem. Commun.* **2009**, 2727–2729; d) S. Mischler, S. Guerra, R. Deschenaux, *Chem. Commun.* **2012**, *48*, 2183–2185.

[3] For examples constructed on a fullerene scaffold, see: a) J. Iehl, R. Pereira de Freitas, B. Delavaux-Nicot, J.-F. Nierengarten, *Chem. Commun.* **2008**, 2450–2452; b) J. Iehl, J.-F. Nierengarten, *Chem. Eur. J.* **2009**, *15*, 7306–7309; c) P. Pierrat, S. Vanderheiden, T. Muller, S. Bräse, *Chem. Commun.* **2009**, 1748–1750; d) J. Iehl, J.-F. Nierengarten, *Chem. Commun.* **2010**, *46*, 4160–4162; e) J.-F. Nierengarten, J. Iehl, V. Oerthel, M. Holler, B. M. Illescas, A. Muñoz, N. Martín, J. Rojo, M. Sánchez-Navarro, S. Cecioni, S. Vidal, K. Buffet, M. Durka, S. P. Vincent, *Chem. Commun.* **2010**, *46*, 3860–3862; f) P. Compain, C. Decroocq, J. Iehl, M. Holler, D. Hazelard, T. Mena Barragán, C. Ortiz Mellet, J.-F. Nierengarten, *Angew. Chem.* **2010**, *122*, 5889; *Angew. Chem. Int. Ed.* **2010**, *49*, 5753–5756; g) M. Durka, K. Buffet, J. Iehl, M. Holler, J.-F. Nierengarten, J. Taganna, J. Bouckaert, S. P. Vincent, *Chem. Commun.* **2011**, *47*, 1321–1323; h) S. Cecioni, V. Oerthel, J. Iehl, M. Holler, D. Goyard, J.-P. Praly, A. Imberty, J.-F. Nierengarten, S. Vidal, *Chem. Eur. J.* **2011**, *17*, 3252–3261; i) P. Fortgang, E. Maisonhaute, C. Amatore, B. Delavaux-Nicot, J. Iehl, J.-F. Nierengarten, *Angew. Chem.* **2011**, *123*, 2412; *Angew. Chem. Int. Ed.* **2011**, *50*, 2364–2367; j) J. Iehl, M. Holler, J.-F. Nierengarten, K. Yoosaf, J. M. Malicka, N. Armaroli, J.-M. Strub, A. Van Dorsselaer, B. Delavaux-Nicot, *Aust. J. Chem.* **2011**, *64*, 153–159; k) M. Sanchez-Navarro, A. Munoz, B. M. Illescas, J. Rojo, N. Martin, *Chem. Eur. J.* **2011**, *17*, 766–769; l) J. Iehl, J.-F. Nierengarten, A. Harriman, T. Bura, R. Ziessel, *J. Am. Chem. Soc.* **2012**, *134*, 988–998; m) J. Iehl, M. Frasconi, H.-P. Jacquot de Rouville, N. Renaud, S. M. Dyar, N. L. Strutt, R. Carmieli, M. R. Wasielewski, M. A. Ratner, J.-F. Nierengarten, J. F. Stoddart, *Chem. Sci.* **2013**, *4*, 1462–1469.

[4] For examples constructed on a polyhedral oligomeric silsesquioxane (POSS) scaffold, see: a) Y. Gao, A. Eguchi, K. Kakehi, Y. C. Lee, *Org. Lett.* **2004**, *6*, 3457–3460; b) Z. Ge, D. Wang, Y. Zhou, H. Liu, S. Liu, *Macromolecules* **2009**, *42*, 2903–2910; c) B. Trastoy, M. E. Pérez-Ojeda, R. Sastre, J. L. Chiara, *Chem. Eur. J.* **2010**, *16*, 3833–3841; d) S. Fabritz, D. Heyl, V. Bagutski, M. Empting, E. Rikowski, H. Frauendorf, I. Balog, W.-D. Fessner, J. J. Schneider, O. Avrutina, H. Kolnar, *Org. Biomol. Chem.* **2010**, *8*, 2212–2218; e) M. Lo Conte, S. Staderini, A. Chambery, N. Berthet, P. Dumy, O. Renaudet, A. Marra, A. Dondoni, *Org. Biomol. Chem.* **2012**, *10*, 3269–3277; f) A. Marra, S. Staderini, N. Berthet, P. Dumy, O. Renaudet, A. Dondoni, *Eur. J. Org. Chem.* **2013**, 1144–1149.

[5] For examples constructed on a macrocyclic core, see: a) E.-H. Ryu, Y. Zhao, *Org. Lett.* **2005**, *7*, 1035–1038; b) S. P. Bew, P. Brimage, N. L'Hermite, S. Sharma, *Org. Lett.* **2007**, *9*, 3713–3716; c) J. Morales-Sanfrutos, M. Ortega-Munoz, J. Lopez-Jaramillo, J. Hernandez-Mateo, F. Santayo-Gonzales, *J. Org. Chem.* **2008**, *73*, 7768–7771; d) S. Cecioni, S. Faure, U. Darbost, I. Bonnamour, H. Parrot-Lopez, O. Roy, C. Taillefumier, M. Wimmerova, J.-P. Praly, A. Imberty, S. Vidal, *Chem. Eur. J.* **2011**, *17*, 2146–2159.

[6] For selected reviews, see: a) H. C. Kolb, M. G. Finn, K. B. Sharpless, *Angew. Chem.* **2001**, *113*, 2056; *Angew. Chem. Int. Ed.* **2001**, *40*, 2004–2021; b) C. Remzi Becer, R. Hoogenboom, U. S. Schubert, *Angew. Chem.* **2009**, *121*, 4998; *Angew. Chem. Int. Ed.* **2009**, *48*, 4900–4908; c) C. E. Hoyle, C. N. Bowman, *Angew. Chem.* **2010**, *122*, 1584; *Angew. Chem. Int. Ed.* **2010**, *49*, 1540–1573; d) G. Franc, A. K. Kakkar, *Chem. Soc. Rev.* **2010**, *39*, 1536–1544; e) C. E. Hoyle, A. B. Lowe, C. N. Bowman, *Chem. Soc. Rev.* **2010**, *39*, 1355–1387.

[7] I. Nierengarten, S. Guerra, M. Holler, J.-F. Nierengarten, R. Deschenaux, *Chem. Commun.* **2012**, *48*, 8072–8074.

[8] T. Ogoshi, S. Kanai, S. Fujinami, T. Yamagishi, Y. Nakamoto, *J. Am. Chem. Soc.* **2008**, *130*, 5022–5023.

[9] For reviews on pillar[*n*]arenes, see: a) P. J. Cragg, K. Sharma, *Chem. Soc. Rev.* **2012**, *41*, 597–607; b) M. Xue, Y. Yang, X. Chi, Z. Zhang, F. Huang, *Acc. Chem. Res.* **2012**, *45*, 1294–1308; c) T. Ogoshi, *J. Inclusion Phenom. Macrocyclic Chem.* **2012**, *72*, 247–262.

[10] a) T. Ogoshi, T. Aoki, K. Kitajima, S. Fujinami, T.-a. Yamagishi, Y. Nakamoto, *J. Org. Chem.* **2011**, *76*, 328–331; b) D. Cao, Y. Kou, J. Liang, Z. Chen, L. Wang, H. Meier, *Angew. Chem.* **2009**, *121*, 9901; *Angew. Chem. Int. Ed.* **2009**, *48*, 9721–9723; c) Y. Kou, H. Tao, D. Cao, Z. Fu, D. Schollmeyer, H. Meier, *Eur. J. Org. Chem.* **2010**, 6464–6470; d) Y. Ma, Z. Zhang, X. Ji, C. Han, J. He, Z. Abliz, W. Chen, F. Huang, *Eur. J. Org. Chem.* **2011**, 5331–5335; e) T. Boinski, A. Szumma, *Tetrahedron* **2012**, *68*, 9419–9422.

[11] M. Holler, N. Allenbach, J. Sonet, J.-F. Nierengarten, *Chem. Commun.* **2012**, *48*, 2576–2578.

[12] a) T. Ogoshi, R. Shiga, M. Hashizume, T.-A. Yamagishi, *Chem. Commun.* **2011**, *47*, 6927–6929; b) H. Zhang, N. L. Strutt, R. S. Stoll, H. Li, Z. Zhu, J. F. Stoddart, *Chem. Commun.* **2011**, *47*, 11420–11422; c) N. L. Strutt, R. S. Forgan, J. M. Spruell, Y. Y. Botros, J. F. Stoddart, *J. Am. Chem. Soc.* **2011**, *133*, 5668–5671; d) H. Deng, X. Shu, X. Hu, J. Li, X. Jia, C. Li, *Tetrahedron Lett.* **2012**, *53*, 4609–4612; e) I. Nierengarten, K. Buffet, M. Holler, S. P. Vincent, J.-F. Nierengarten, *Tetrahedron Lett.* **2013**, *54*, 2398–2402.

[13] It is known that isolated molecules with point groups displaying fivefold symmetry must reduce their symmetry when forming crystalline monolayers, see: T. Bauert, L. Merz, D. Bandera, M. Parschau, J. S. Siegel, K.-H. Ernst, *J. Am. Chem. Soc.* **2009**, *131*, 3460–3461.

[14] Y. Ma, X. Ji, F. Xiang, X. Chi, C. Han, J. He, Z. Abliz, W. Chen, F. Huang, *Chem. Commun.* **2011**, *47*, 12340–12342.

[15] H. Tao, D. Cao, L. Liu, Y. Kou, L. Wang, H. Meier, *Sci. China Chem.* **2012**, *55*, 223–228.

[16] Compound **7** has already been prepared by following another synthetic route, see: X.-B. Hu, L. Chen, W. Si, Y. Yu, J.-L. Hou, *Chem. Commun.* **2011**, *47*, 4694–4696.

[17] Related stabilization of mesophases has also been observed for metallomesogens, see: a) K. Binemans, Y. G. Galymetdinov, R. Van Deun, D. W. Bruce, S. R. Collinson, A. P. Polishchuk, I.

Bikchantaev, W. Haase, A. V. Prosvirin, L. Tinchunira, I. Litvinov, A. Gubajdullin, A. Rakhmatullin, K. Uyttterhoeven, L. Van Meerlet, *J. Am. Chem. Soc.* **2000**, *122*, 4335–4344; b) J.-F. Eckert, U. Maciejczuk, D. Guillon, J.-F. Nierengarten, *Chem. Commun.* **2001**, 1278–1279; c) K. Binnemas, K. Lodewyckx, *Angew. Chem.* **2001**, *113*, 248; *Angew. Chem. Int. Ed.* **2001**, *40*, 242–244; d) K. Binnemas, C. Gorller-Walrand, *Chem. Rev.* **2002**, *102*, 2303–2345.

[18] a) G. J. Brownsey, A. J. Leadbetter, *J. Phys. Lett.* **1981**, *42*, 135–140; b) B. Dardel, D. Guillon, B. Heinrich, R. Deschenaux, *J. Mater. Chem.* **2001**, *11*, 2814–2831.

[19] a) P. Davidson, A. M. Levelut, M. F. Achard, F. Hardouin, *Liq. Cryst.* **1989**, *4*, 561–571; b) J. Barberá, L. Giorgini, F. Paris, E. Salatelli, R. M. Tejedor, L. Angiolini, *Chem. Eur. J.* **2008**, *14*, 11209–11221.

[20] S. Frein, F. Camerel, R. Ziessel, J. Barberá, R. Deschenaux, *Chem. Mater.* **2009**, *21*, 3950–3959.

[21] B. Dardel, D. Guillon, B. Heinrich, R. Deschenaux, *J. Mater. Chem.* **2001**, *11*, 2814–2831.